

Efficient Removal of Ni(II) from Aqueous Solution by Date Seeds Powder Biosorbent: Adsorption Kinetics, Isotherm and Thermodynamics

Authors:

Abubakr Elkhaleefa, Ismat H. Ali, Eid I. Brima, A. B. Elhag, Babiker Karama

Date Submitted: 2020-12-22

Keywords: thermodynamics, isotherm, kinetics, date seeds, Adsorption

Abstract:

Adsorption investigations in batch approaches were performed to explore the biosorption of Ni(II) ions from aqueous solutions on date seeds powder. The effects of pH, particle size, initial concentration of Ni(II) ions, adsorbent mass, temperature, and contact on the adsorption efficacy were studied. The maximum removal obtained was 90% for an original Ni(II) ion solution concentration of 50 ppm was attained at pH 7 after 30 min and with 0.30 g of an added adsorbent. The four adsorption models, namely Freundlich, Langmuir, Dubinin-Radushkevich (D-R), and Temkin were examined to fit the experimental findings. The adsorption system obeys the Freundlich model. The system was found to follow the pseudo-second order kinetic model. Thermodynamic factors; entropy (ΔS°), enthalpy (ΔH°), and Gibbs free energy (ΔG°) changes were also assessed. Results proved that adsorption of Ni(II) ions is exothermic and spontaneous. Sticking probability value was found to be less than unity, concluding that the process is dominated by physical adsorption.

Record Type: Published Article

Submitted To: LAPSE (Living Archive for Process Systems Engineering)

Citation (overall record, always the latest version):

LAPSE:2020.1276

Citation (this specific file, latest version):

LAPSE:2020.1276-1

Citation (this specific file, this version):




LAPSE:2020.1276-1v1

DOI of Published Version: <https://doi.org/10.3390/pr8081001>

License: Creative Commons Attribution 4.0 International (CC BY 4.0)

Article

Efficient Removal of Ni(II) from Aqueous Solution by Date Seeds Powder Biosorbent: Adsorption Kinetics, Isotherm and Thermodynamics

Abubakr Elkhaleefa ^{1,2} , Ismat H. Ali ^{3,*} , Eid I. Brima ^{3,4} , A. B. Elhag ^{5,6}
and Babiker Karama ⁷

¹ Department of Chemical Engineering, College of Engineering, King Khalid University, Abha 61413, Saudi Arabia; amelkhalee@kku.edu.sa

² Department of Chemical Engineering and Chemical Technology, University of Gezira, Wadmedani 21113, Sudan

³ Department of Chemistry, College of Science, King Khalid University, Abha 61413, Saudi Arabia; ebrima@kku.edu.sa

⁴ School of Allied Health Science, De Montfort University, The Gateway, Leicester LE1 9BH, UK

⁵ Department of Civil Engineering, College of Engineering, King Khalid University, Abha 61413, Saudi Arabia; abalhaj@kku.edu.sa

⁶ Department of Geology, Faculty of Science, Kordofan University, Elobied 51111, Sudan

⁷ Department of Chemical Engineering, Karary University, Khartoum 14411, Sudan; babikerka@hotmail.com

* Correspondence: ihali@kku.edu.sa

Received: 20 July 2020; Accepted: 14 August 2020; Published: 17 August 2020



Abstract: Adsorption investigations in batch approaches were performed to explore the biosorption of Ni(II) ions from aqueous solutions on date seeds powder. The effects of pH, particle size, initial concentration of Ni(II) ions, adsorbent mass, temperature, and contact on the adsorption efficacy were studied. The maximum removal obtained was 90% for an original Ni(II) ion solution concentration of 50 ppm was attained at pH 7 after 30 min and with 0.30 g of an added adsorbent. The four adsorption models, namely Freundlich, Langmuir, Dubinin–Radushkevich (D–R), and Temkin were examined to fit the experimental findings. The adsorption system obeys the Freundlich model. The system was found to follow the pseudo-second order kinetic model. Thermodynamic factors; entropy (ΔS°), enthalpy (ΔH°), and Gibbs free energy (ΔG°) changes were also assessed. Results proved that adsorption of Ni(II) ions is exothermic and spontaneous. Sticking probability value was found to be less than unity, concluding that the process is dominated by physical adsorption.

Keywords: adsorption; date seeds; kinetics; isotherm; thermodynamics

1. Introduction

The presence of heavy metals in water streams is among one of the most dangerous environmental problems arising from the disposal of untreated industrial effluents [1–4]. Many industries comprise of final treatment processes where discharged metal compounds may lead to pollution in the effluent water [2,5,6]. Most of these heavy metals are non-biodegradable or with long biological half-life leading to potential accumulation and human exposure through food or water [1].

Ni(II) ions exist naturally in water as nitrates, sulfides, and oxides. Nickel intake above the permissible limit causes skin dermatitis, fibrosis, vomiting, pulmonary, nausea, and many other diseases [3,6–9]. Most of the methods used for Ni(II) removal from artificial wastewater-like cation exchange and precipitation are costly and produce toxic sludge [2,9]. Recently, some economical, renewable, and effective agricultural and natural materials have been studied as alternative biosorbents [2].

Date (*Phoenix dactylifera*) seeds, which are composed of lignin, hemicellulose, and cellulose are effective biosorbents; thus, eliminates various contaminants from wastewater [4,10]. The efficiency of this inexpensive biosorbent is due to oxygenated functional groups in the lignocellulosic materials such as cellulose and phenolic compounds [10]. The removal of Ni(II) ions onto bentonite/grapheme oxide was previously studied [11] and the results revealed that it follows Langmuir isotherm with high uptake capacity. Mehrmad et al. [12] have reported that the removal of Ni(II) ions by functionalized henna powder depends on the experimental circumstances, mainly the Ni(II) concentration, the biosorbent mass, and the pH of the medium, the Freundlich and Langmuir isotherm models were used to define the process. The kinetic data were fitted with the pseudo-second-order reaction. The adsorption of Ni(II) ions from wastewater by natural clay had previously been investigated [13] and it was reported that the process is controlled by the pH value of the medium; the sorption process was rapid whereas the maximum adsorption capacity had been attained within 120 min and it was found that the system follows a pseudo-second-order reaction.

The adsorbent used in this study was prepared by a direct, facile, and economic technique. The process does not require any chemicals addition nor high-temperature calcination. It is believed that only few adsorbents were tested without any modification in the removal of heavy metals from aqueous solutions while being powerfully recyclable. *Phoenix dactylifera* is one of the most plentiful plants in Saudi Arabia and the region. Using date seed powder as an adsorbent for Ni(II) ions is considered the novelty of this research.

This work aims to assess the potential of date seed powder to act as an inexpensive and environment-friendly material for the removal of Ni(II) from artificial wastewater. This study was designed to assess, compare, and characterize the adsorption of Ni(II) ions by date seeds powder (DSP) without the addition of any chemicals or thermal treatment. DSP was initially characterized using Brunauer–Emmett–Teller (BET) surface area, scanning electron microscope technique (SEM), and attenuated total reflection-Fourier transform infrared spectrometer (ATR-FTIR). The factors that influence the adsorption efficiency such as mass, concentration of Ni(II) ion, pH, temperature, and contact time, were investigated in this work.

2. Materials and Methods

2.1. Collection and Treatment of Adsorbent

Dates seeds were collected locally from Abha city, Saudi Arabia. Seeds were rinsed with tap water and then by deionized water, dried at room temperature and were then grounded to powder size using a ball mill before being sieved. The efficiency of the room-temperature dried DSP was compared with small amount of oven-dried DSP and no differences were noticed on the results. Thus, to minimize the cost, drying of DSP by oven was not used in this study.

2.2. Reagents

Deionized water ($>18 \Omega/\text{cm}$, Milli-Q) was used throughout this work for the solutions and DSP preparations. A stock solution of 1000 ppm Ni(II) ions was prepared using NiNO_3 (LOBA Chemie, Laboratory Reagents and fine Chemicals, Mumbai, India).

2.3. Batch Adsorption

Adsorption batch experiments were conducted at different operating conditions (pH, time, adsorbent dosage, adsorbent particles size, and temperature) by adding the desired amount of DSP to 50 mL of Ni(II) ion solution under each particular condition. NaOH (0.25 M) and/or HCl (0.25 M) were used to control the pH value. Mechanical thermostated shaker (WSB, Witeg, Belrose, Germany) was used throughout all the experiments. The solutions were filtered and then analyzed using Atomic

Absorption Spectroscopy (AAS) (SpectrAA 220, Varian, Australia) to measure the remaining Ni(II) ions concentrations. The removal efficiencies (R%) were calculated using Equation (1).

$$R\% = \frac{C_0 - C_e}{C_0} \times 100 \quad (1)$$

where C_0 and C_e are the initial and equilibrium Ni(II) ion concentrations, respectively.

2.4. Characterization of Biosorbent

The Brunauer–Emmett–Teller (BET) surface area, pore size and pore volume after and before the adsorption process were investigated using Quanta Chrome NOVA 4200E Surface Area Analyzer. The morphology of the DSP was investigated using a scanning electron microscope technique (SEM) JEOL 6360 (Japan). Accelerating voltage of 20 kV was used. The functional groups of DSP before and after the adsorption process were investigated by ATR-FTIR (Cary 630 FTIR from Agilent) in the range of 4000–400 cm^{-1} at a spectral resolution of 8 cm^{-1} . DSP samples were analyzed without any pretreatment.

3. Results and Discussion

3.1. Characterization of the DSP

Table 1 displays the results of the analysis of DSP by surface area analyzer. Results prove that DSP poses a mesoporous arrangement. Mesopores are detected over the entire sample surface forming a highly uniform and interpenetrating permeable media. Moreover, results also confirm that DSP has a large surface area compared to some other adsorbents used to adsorb Ni(II) ions [13].

Table 1. Properties of the DSP surface.

Surface Area (m^2/g)	Total Pore Volume (cm^3/g)	Average Pore Diameter (Å)
124	46.9×10^{-2}	98

3.2. ATR—FTIR Spectrum

Investigations of the ATR-FTIR spectra from DSP after and before the adsorption process (Figure 1) proves the presence of functional groups, which are among the major characteristic to DSP. The presence of developed aliphatic groups was identified by the absorption band ascribed to the stretching vibrations of carbon-hydrogen bonds in the range between (2980–2840 cm^{-1}). OH functional groups were recognized by the broad band ascribed to stretching vibrations of oxygen-hydrogen bonds in the range from 3600 to 3100 cm^{-1} , whereas, ether structures were identified by the band ascribed to stretching vibrations of carbon-oxygen in the range (1100–1000 cm^{-1}). Moreover, CO groups were also detected by the band ascribed to stretching vibrations of C=O bonds in the range from 1750 to 1500 cm^{-1} . On the other hand, the bands of aromatic compounds bond groups overlay with those obtained by the bonds of other structures. Generally, the FTIR spectrum proves the multiplicity of the structure of DSP. The presence of these aforementioned functional groups on the DSP surface indicates its potential ability to act as a promising adsorbent [14].

3.3. Scanning Electron Microscope Technique (SEM)

The SEM technique investigations provided an insight into the diverse morphology of the DSP where some larger constituents show asymmetrical form, some other constituents have an extended rod-like construction whereas other smaller constituents display rectangular form. Overall, most of the constituents have a reedy and coarse structure with irregular ends. Particle size of the DSP ranges from 5–15 μm . It can be noted from Figure 2a the availability of numerous available cavities and holes

enabling Ni(II) ions to be adsorbed, while Figure 2b shows that these holes are occupied by Ni(II) ions indicating good adsorption capacity for DSP.

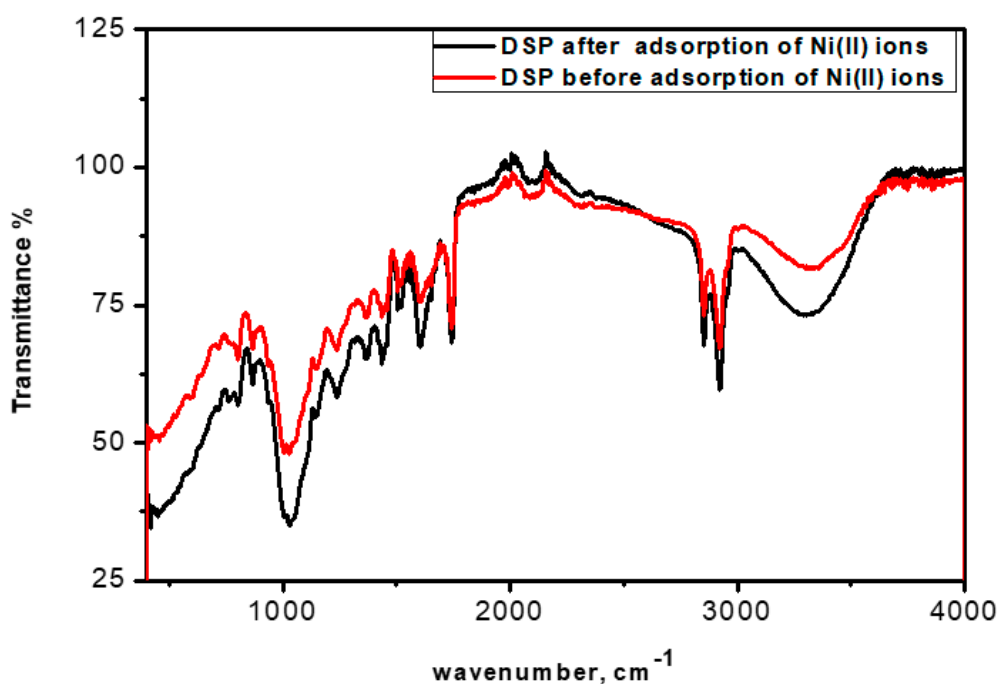


Figure 1. Attenuated total reflection-Fourier transform infrared spectrometer (ATR-FTIR) spectra for the date seeds powder (DSP) before and after Ni(II) ions adsorption process.

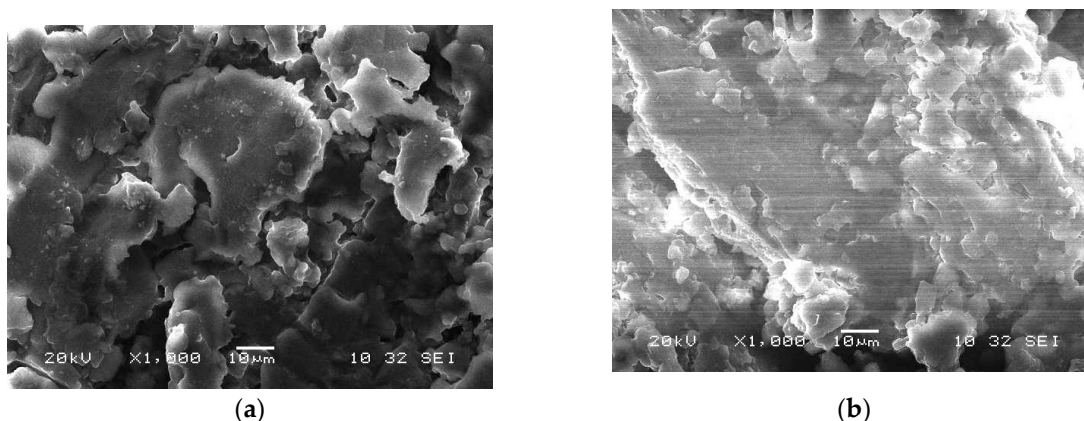


Figure 2. SEM technique images of the DSP surface (a) before and (b) after adsorption.

3.4. Effect of pH Values

A pH range of 1–11 was assessed to define the optimum value for the removal of Ni(II) ions by adsorption. Results are presented in Figure 3. It has been noted that the adsorption efficiency increases with increasing pH value up to 7, after which no alteration was noted with further increase in the pH value. These results attributed to the competition between Ni(II) ions and H⁺ ions for adsorption spots on the DSP surface at low pH values [15]. As the pH value increases, less H⁺ ions are present; hence, more adsorption sites are available for Ni(II) ions. The optimal pH value was defined as 7; thus, been used throughout this work.

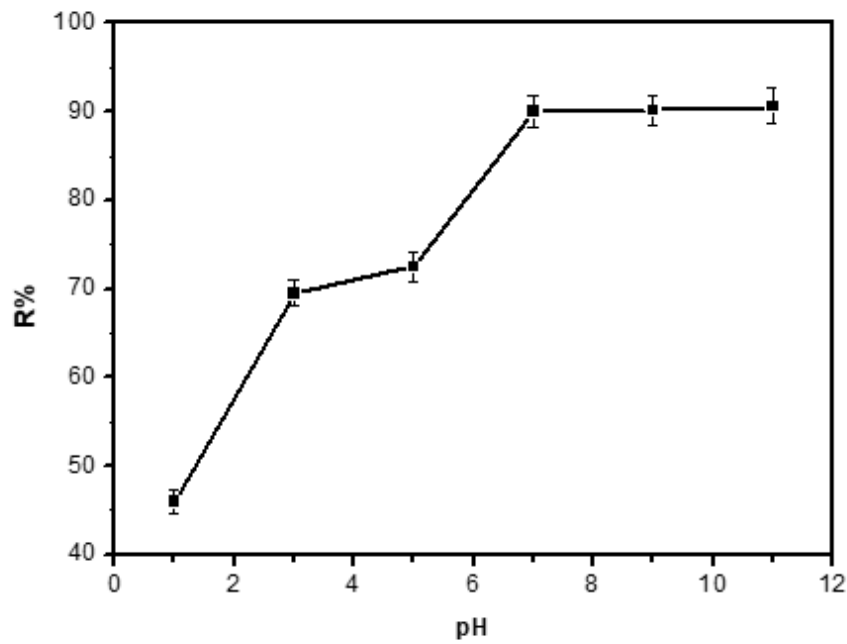


Figure 3. Effect of changing pH values on the efficiency of removal of Ni(II) ions.

3.5. Effect of Adsorbent Particle Size

Different particle sizes ranging from 100, 150, 250, 400, and 600 μm have been examined and the obtained results (Figure 4) showed that as the particle size decreases, the removal amount increases from 82% to 90%. This is due to the availability of more surface area obtainable for the removal of Ni(II) ions as the particle size decreases. However, no difference in adsorption was observed with particle sizes of 100 and 150 μm . Particle size of 100 μm was used throughout the study.

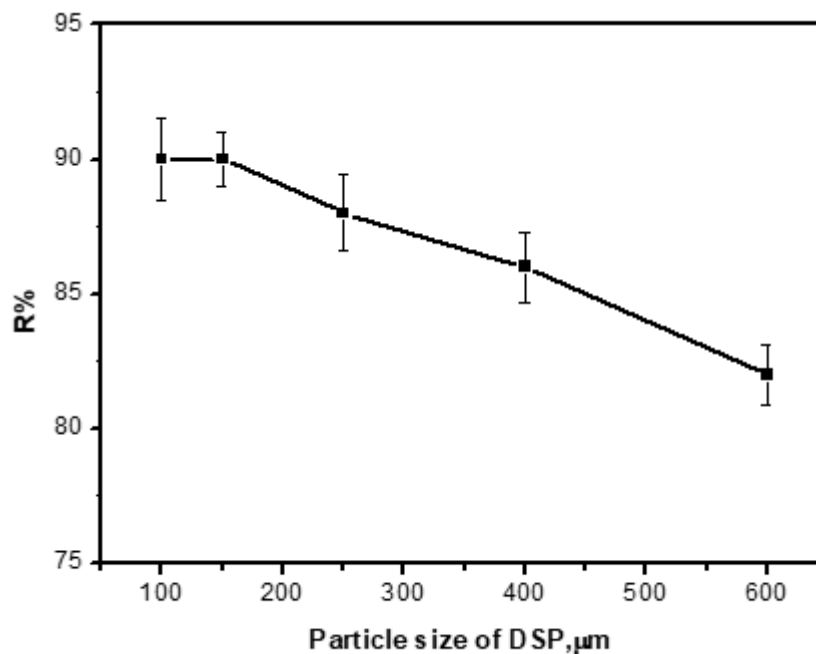


Figure 4. Effect of particle size of the DSP on the efficiency of removal of Ni(II) ions.

3.6. Effect of Adsorbent Mass

The dependence of the adsorption efficiency on DSP mass was studied to determine the optimal mass. Results displayed in Figure 5 show that the removal efficiency of Ni(II) ions increased as the DSP mass increases from 0.05 g to 0.30 g. Increasing the DSP mass to more than 0.30 g has no significant effect on adsorption effectiveness. This is due to the fact that the surface area of the adsorbent increases with its mass. The optimal DSP mass (0.30 g) was throughout this study.

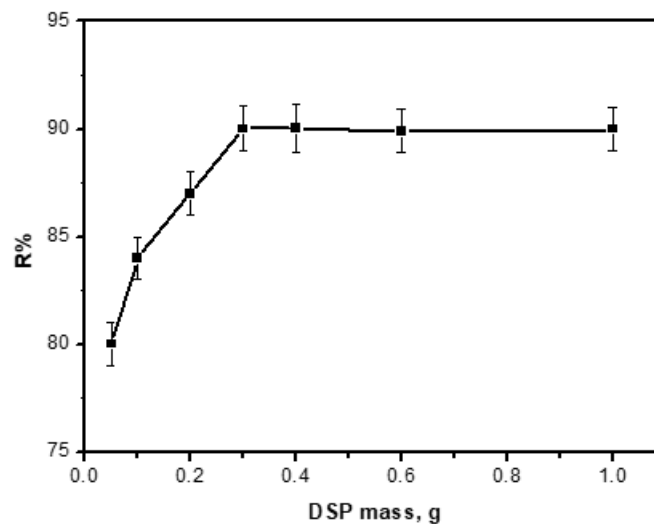


Figure 5. Effect of the DSP mass on the removal efficiency of Ni(II) ions.

3.7. Effect of Contact Time

In typical contaminant removal experiments, the contact time is considered a significant feature because it directly influences the adsorbent lifetime and the adsorption efficiency. Figure 6 shows the results obtained at different time intervals while all the other conditions (pH = 7.00, particle size = 100 μm , adsorbent mass = 0.30 g and temperature = 25.0 $^{\circ}\text{C}$, revolutions per minute (rpm) = 150) were kept constant. It was found that the DSP reached the maximum adsorption of 90% for Ni(II) after 30 min.

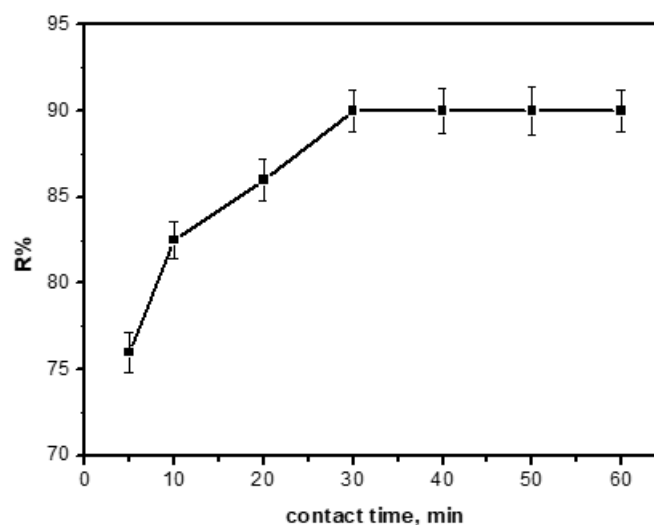


Figure 6. Effect of contact time on the efficiency of removal of Ni(II) ions.

3.8. Adsorption Kinetics

Kinetics of the adsorption process is the key feature for designing efficient adsorption experiments and this requires the use of proper kinetic model. Several kinetic parameters values are shown in Table 2. Adsorption kinetics control the rate, g the efficacy of DSP [16]. Several kinetic models were examined such as intraparticle diffusion, pseudo-second-order model, and pseudo-first-order.

Table 2. Kinetic parameters for the removal of Ni(II) ion by DSP.

Kinetic Models	Parameters	
Pseudo-first-order model	q_e (mg/g)	12.2
	k_1 (min^{-1})	4.0×10^{-4}
	R^2	0.6988
Pseudo-second-order model	q_e (mg/g)	3.1
	k_2 (g/mg min)	0.3
	R^2	0.9937
Intraparticle diffusion model	k_{id} (mg/g. $\text{min}^{(1/2)}$)	0.056
	I	2.6
	R^2	0.7978

3.8.1. Pseudo-First-Order Model

This model is denoted by Equation (2) [17].

$$\ln(q_e - q_t) = \ln q_e - k_1 t \quad (2)$$

The pseudo-second order kinetic model is denoted by Equation (3).

$$\frac{t}{q_t} = \frac{1}{k_2 q_e^2} + \frac{t}{q_e} \quad (3)$$

where q_e and q_t are the equilibrium and adsorption capacities at time (t) and equilibrium, and k_1 , k_2 are rate constants for pseudo-first-order and pseudo-second-order, respectively. Moreover, 0.6977 and 0.9937 are values of correlation coefficients (R^2) for pseudo-first-order and pseudo-second-order models (Table 2), respectively. Figure 7 proves that the system obeys the pseudo-second-order kinetics model. This is in good agreement with previous studies [12,13,15].

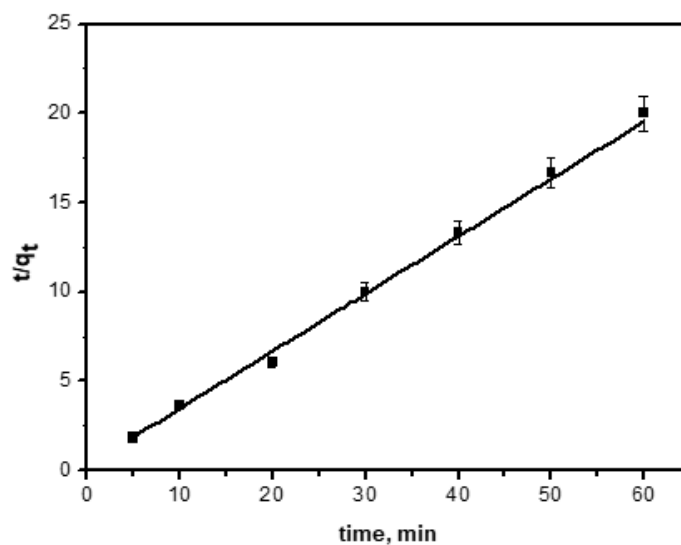


Figure 7. Pseudo-second-order kinetics.

3.8.2. Intra-Particle Diffusion Kinetic Model

Intra-particle diffusion kinetic model is displayed by Equation (4)

$$q_t = k_{id} t^{1/2} + I \quad (4)$$

k_{id} is the intra-particle diffusion rate constant ($\text{mg/g} \cdot \text{min}^{(1/2)}$) and I is a constant that associated to the boundary layer thickness (mg/g). The value of (k_{id}) was determined from the slope of Equation (4) and presented in Table 2. The relationship between q_t and $t_{1/2}$ was non-linear, demonstrating that several processes are governing the adsorption process. The initial curved portion of the plot is due to the impact of boundary layer diffusion. The curved portion denotes that the intra-particle diffusion is controlled by the rate of constant k_{id} .

3.9. Adsorption Isotherm

Adsorption models are frequently exploited to explain the adsorbate/adsorbent interactions to determine the adsorption capacity of the adsorbent. To evaluate the adsorption isotherms for the DSP, Freundlich, Langmuir, Temkin, and Dubinin–Radushkevich (D–R) adsorption models were examined.

3.9.1. Langmuir Model

Equation (5) presents the Langmuir linear equation

$$\frac{C_e}{q_e} = \frac{C_e}{q_m} + \frac{1}{bq_m} \quad (5)$$

where q_e is the equilibrium quantity of Ni(II) ions adsorbed on the DSP surface at equilibrium (mg/g), C_e is the equilibrium concentration of Ni(II) ions in solution (mg/L), q_m is the maximum adsorption of Ni(II) ions (mg/g), and b (L/mg) is the Langmuir constant. According to Equation (4), values of C_e/q_e were plotted against C_e and the results are displayed in Figure 8a. Values of q_m and b were obtained from the slope and intercept, respectively. The b value refers to the adsorption binding energy [14], whereby a higher b value means more binding affinity between adsorbent and adsorbate. The parameters (q_m , b and R^2) are displayed in Table 3.

Table 3. Parameters obtained from various isotherm models.

Adsorption Model	Isotherm Constants	Value
Langmuir	q_{\max} (mg/g)	40.8
	K_L (L/g)	0.029
	R^2	0.887
Freundlich	N	0.67
	K_f ($(\text{mg/g})/(\text{mg/L})^n$)	4.6
	R^2	0.9981
Temkin	A (L/g)	2.1
	b_t (kJ/mol)	370.3
	R^2	0.899
D-R	β	2.0×10^{-7}
	q_m (mg/g)	7.18
	R^2	0.846

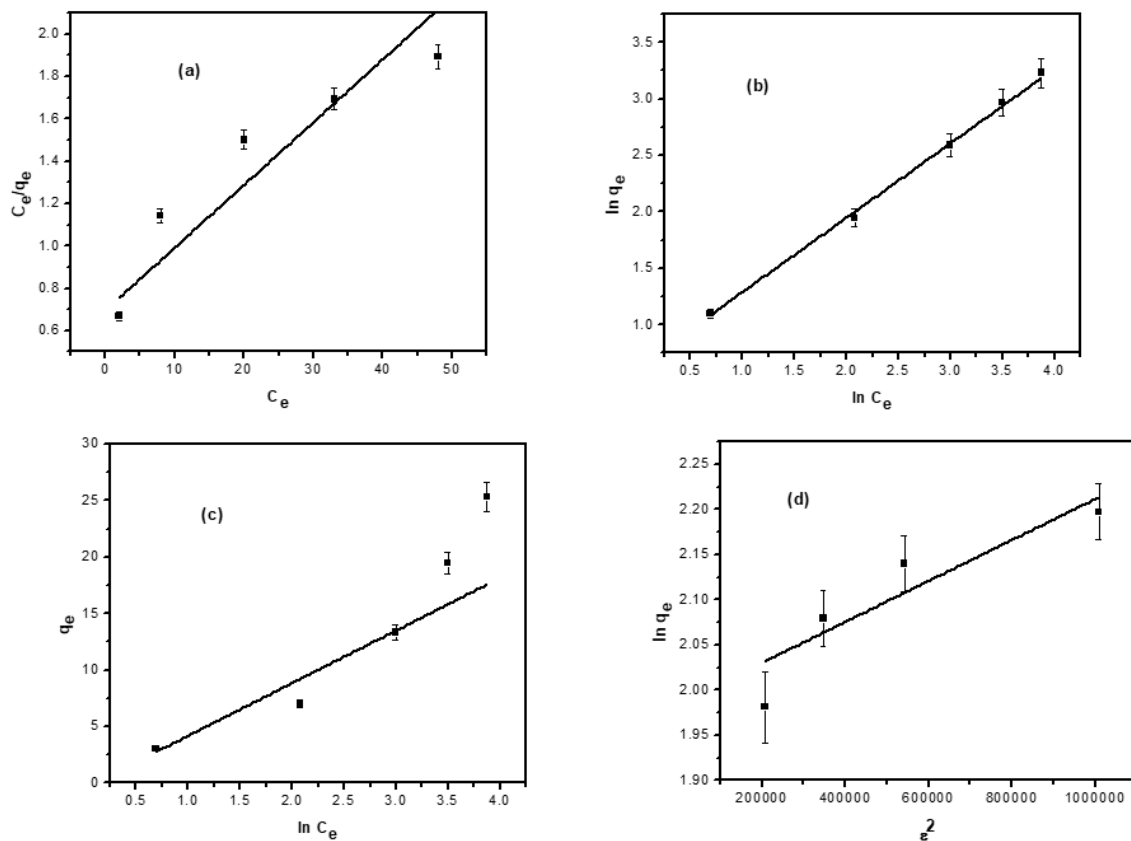


Figure 8. Isotherm models of adsorption of Ni(II) ions by the DSP (a), Langmuir, (b) Freundlich, (c) Temkin and (d) D-R.

3.9.2. Freundlich Model

This is an experimental association relating the adsorption of solutes from a liquid onto an adsorbent surface and adopts that various adsorption layers with a number of adsorption energies are involved. This model describes the affinity between the quantities of Ni(II) ions adsorbed per the dosage of the DSP, q_e , and the concentration of the Ni(II) ions at equilibrium, C_e . Linear Freundlich model is represented by Equation (6) [12].

$$\ln q_e = \ln K_f + \frac{1}{n} \ln C_e \quad (6)$$

where n and K_f represent Freundlich constants describe the process intensity capacity. Values of K_f and n are obtained from the intercept and slope of Figure 8b, respectively. Value of n is an indicator to the adsorption nature according to the following way: if $n < 1$, adsorption is classified as a physical process, if $n = 1$, adsorption is linear and if $n > 1$, adsorption is considered as a chemical process. The range of n values and K_f value are given in Table 3. Results indicate that adsorption of Ni(II) ion on the surface of the DSP is a physical process [13].

3.9.3. Temkin Isotherm

Temkin model proposes that the adsorption heat of all particles in the layer decrease sharply, rather than logarithmic with coverage [18]. The adsorption potential of DSP to Ni(II) ions can be verified by applying Temkin isotherm model. The linear formula of Temkin is shown in Equation (7):

$$q_e = \frac{RT}{b_t} \ln A + \frac{RT}{b_t} \ln C_e \quad (7)$$

where R is the universal gas constant, T is the absolute temperature, b_t is Temkin constant associated with adsorption heat, and A is a constant related to adsorption capacity. A and b_t values are found from the slope and intercept of Figure 8c and given along with R^2 in Table 3.

3.9.4. Dubinin–Radushkevich (D–R) Isotherm Model

This model estimates the energy of adsorption. It is commonly used to understand the mechanism of adsorption [19]. This isotherm is not proposed only for constant adsorption potential or homogeneous adsorbent but also for both heterogenous surfaces. The linear equation of this model is presented in Equation (8):

$$\ln q_e = \ln q_m - \beta \epsilon^2 \quad (8)$$

ϵ is given by Equation (9):

$$\epsilon = RT \ln \left(1 + \frac{1}{C_e} \right) \quad (9)$$

β is a constant associated with the adsorption free energy, q_m is the theoretical saturation capacity based on D–R isotherm (mg/g). Values of β , q_m and R^2 are obtained from Figure 8d and shown in Table 3. The free sorption energy E_s , is the change in free energy when one mole of adsorbate is stimulated to the solid surface and is calculated by Equation (10).

$$E_s = \frac{1}{\sqrt{2\beta}} \quad (10)$$

The adsorption type can be deduced from the E_s value. The adsorption process is considered chemical when E_s value is in the range 8.0 to 16.0 kJ/mol and physical when E_s is less than 8.0 kJ/mol. In this work, the E_s value was determined as 2.24 kJ/mol concluding that the adsorption taking action is of physical nature.

3.10. Effect of Temperature

Figure 9 displays the influence of temperature on the adsorption of Ni(II) ions onto the DSP surface. The adsorption efficiency decreases as the temperature increases. This is justified due to the damage of some adsorption sites at elevated temperatures.

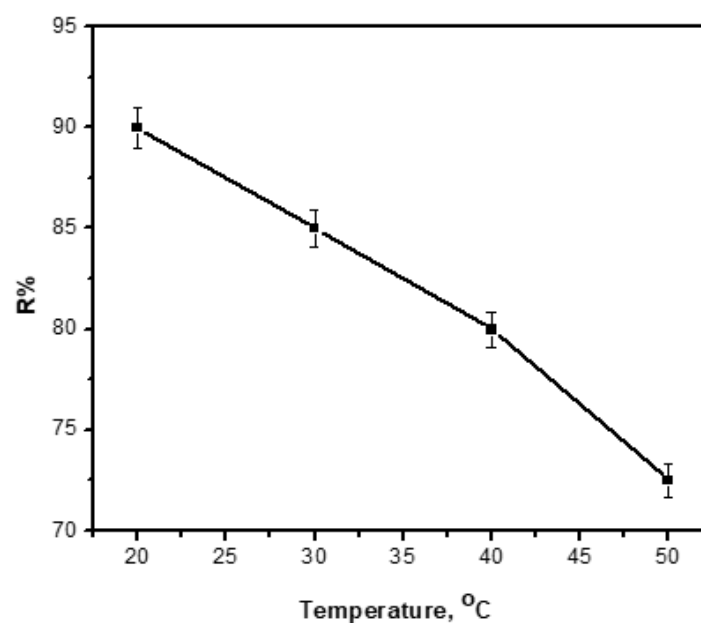


Figure 9. Effect of temperature on the removal efficiency of Ni(II) ions by the DSP.

3.11. Adsorption Thermodynamics

Thermodynamical parameters are vital in any adsorption investigations as the temperature is strongly connected to the kinetic energy of adsorbate. In this study, adsorption tests were performed at different temperatures, viz. 298, 308, 318 and 328 K for the sorption of initial Ni(II) ion concentration (50 mg/L) on DSP at their particular optimum pH values, DSP mass and contact time. Entropy (ΔS°), enthalpy (ΔH°), and Free energy (ΔG°) change are governed by Equations (11) and (12).

$$\Delta G^\circ = RT \ln K_D \quad (11)$$

$$\ln K_D = \frac{-\Delta H^\circ}{RT} + \frac{\Delta S^\circ}{R} \quad (12)$$

where K_D value were calculated by Equation (13)

$$K_D = \frac{q_e}{C_e} \quad (13)$$

The thermodynamical parameters are listed in Table 4. Negative signs of ΔG° indicate that the process is spontaneous. It is clear that the negative values of ΔG° decrease as the temperature increases. This is attributed to the fact that additional positions on the surface of the DSP are destroyed at elevated temperatures. Values of ΔG° for Ni(II) ions adsorption onto the DSP were found in the range of -3.5 to -5.7 kJ/mol. It is well established that physical adsorption free energy change (ΔG°) is ranging between -20 and 0 kJ/mol and chemical adsorption between -400 to -80 kJ/mol [13]. Thus, adsorption process is mainly a physical sorption process. This finding is in good agreement with the parameters obtained from Freundlich, Dubinin–Radushkevich (D-R) and Temkin models. ΔS° and ΔH° were calculated from the intercept and slope of Figure 10 and presented in Table 3. The negative value of ΔH° (-27.0 kJ/mol) proves that the adsorption is an exothermic process. The positive value of ΔS° (71.0 J/mol) designates the affinity of the DSP towards the Ni(II) ions.

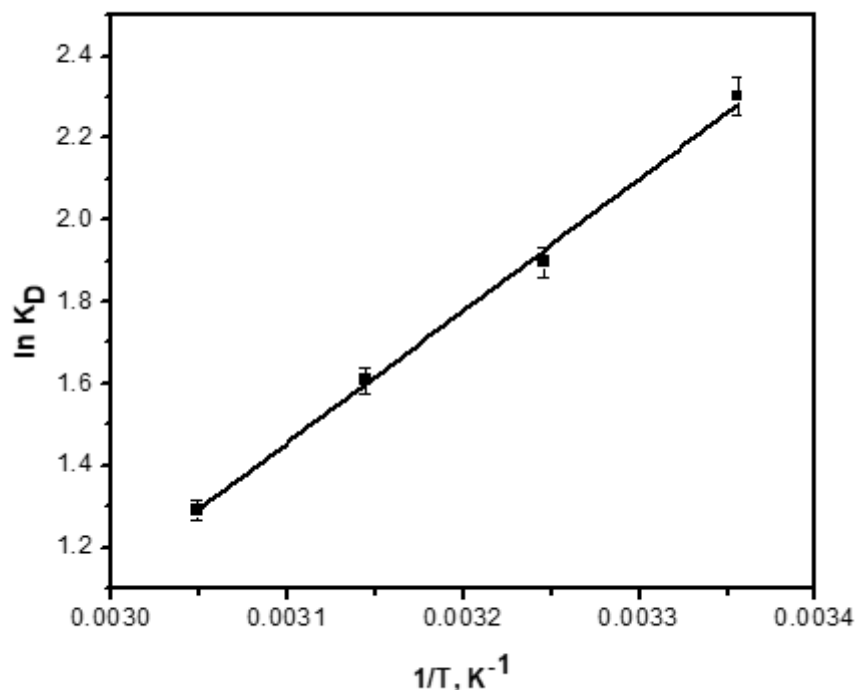


Figure 10. Relationship between $\ln K_D$ and $1/T$.

Values of sticking probability (S^*) and activation energy (E_a) were calculated by applying the modified Arrhenius equation that shown in Equations (14) and (15) [19]:

$$S^* = (1 - \theta)e^{\frac{-E_a}{RT}} \quad (14)$$

$$\theta = \left(1 - \frac{C_e}{C_i}\right) \quad (15)$$

where θ is the surface coverage, C_i represents the original concentration of Ni(II) ions, E_a is the activation energy of the system and S^* is the sticking probability.

The sticking probability, S^* , is a function of the adsorbent/adsorbate adsorption process but should fulfil the circumstance $0 < S^* < 1$ and depends on the temperature of the process. E_a and S^* values were obtained from the slope and intercept of Figure 10, and are recorded in Table 4. The E_a value is very low (-2.01 kJ/mol) demonstrating the facile adsorption process and the negative charge of E_a value indicates an exothermic process. This is in good agreement with the negative value of ΔH° [15]. Since the value of $S^* \ll 1$, therefore, the probability of Ni(II) ion to stick on the DSP is very high and thus the adsorption process is favorable [18].

Table 4. Values of thermodynamic parameters.

T, K	K_D	ΔG° (kJ/mol)	ΔS° (J/mol K)	ΔH° (kJ/mol)	E_a (kJ/mol)	S^* (J K/mol)
298	10.0	-5.7				
308	6.7	-4.9	71.7	-27.0	-2.01	0.002
318	5.0	-4.2				
328	3.6	-3.5				

3.12. Comparisons with Other Adsorbents

Table 5 presents the results of this study compared with other biosorbents. Under the same experimental conditions in terms of optimum pH, temperature, DSP proved high adsorption efficiency in contrast to the chosen biosorbents. It is interesting to note that the DSP was used without any further chemical or thermal modifications. This reduces its cost and hazard to the minimum.

Table 5. Comparison of the DSP with other biosorbents used for the removal of Ni(II) ions.

Biosorbent	q_m (mg/g)	Isotherm Model	Kinetic Model	Optimal pH	Reference
Date seeds powder	41.0	Freundlich	2nd order	7.00	This study
Aloe barbadensis Miller leaves	10.0	Freundlich	2nd order	3.00	[20]
peel of Artocarpus nobilis fruit	12.1	Langmuir	**	4.00	[21]
Modified Aloe barbadensis leaves	29.0	Langmuir	2nd order	7.00	[22]
brown algae Sargassum sp.	1.3	Langmuir	2nd order	6.50	[23]
Calotropis procera roots	0.6	Langmuir	**	3.00	[24]
Peat	61.3	Langmuir	2nd order	9.00	[14]
Barely straw	35.8	Langmuir	**	4.85	[25]
Orange peel	162.6	Langmuir	2nd order	5.50	[26]
Tea factory waste	18.4	Langmuir	**	4.00	[27]

** not reported.

4. Conclusions

In this study, the powder obtained from date seeds has been tested as a competent (removal effectiveness > 90%), inexpensive, eco-friendly and natural material for adsorption of Ni(II) ions from artificial wastewater. The date seeds powder retained significant amounts of Ni(II) readily. The maximum adsorption capacity for DSP was found to be 41 mg/g. The optimal conditions for efficient removal of 50 ppm of Ni(II) ion were found to be 0.30 g of DSP after 30 min of shaking time

at pH 7.00. This adsorbent has positive characteristics making it appropriate to purify wastewater. Such characteristics include (i) cost-effective material: date seeds powder is an expensive material. The only cost of this material would be for the collection, transportation and grinding. It does not need any further chemical or thermal modification (ii) availability: date seeds are abundantly existing in Saudi Arabia (iii) efficiency: date seeds powder can remove more than 90% of Ni(II) ions, which present in artificial wastewater.

Author Contributions: Conceptualization I.H.A. and A.E.; methodology, A.E.; validation, E.I.B.; formal analysis, E.I.B.; investigation A.E.; resources, A.B.E.; writing—original draft preparation, I.H.A. and A.E.; writing—review and editing, E.I.B.; supervision, B.K.; project administration, I.H.A.; funding acquisition, A.B.E. All authors have read and agreed to the published version of the manuscript.

Funding: This research was funded by DEANSHIP OF SCIENTIFIC RESEARCH, KING KHALID UNIVERSITY, grant number R.G.P.1/139/40.

Conflicts of Interest: The authors declare no conflict of interest.

References

- Kulkarni, R.M.; Shetty, K.V.; Srinikethan, G. Cadmium (II) and nickel (II) biosorption by *Bacillus laterosporus* (MTCC 1628). *J. Taiwan Inst. Chem. Eng.* **2014**, *45*, 1628–1635. [[CrossRef](#)]
- Putra, W.P.; Kamari, A.; Yusoff, S.N.M.; Ishak, C.F.; Mohamed, A.; Hashim, N.; Isa, I.M. Biosorption of Cu (II), Pb (II) and Zn (II) ions from aqueous solutions using selected waste materials: Adsorption and characterisation studies. *J. Encapsul. Adsorpt. Sci.* **2014**, *4*, 720–726.
- Karatas, M. Removal of Pb(II) from water by natural zeolitic tuff: Kinetics and thermodynamics. *J. Hazard. Mater.* **2012**, *199*, 383–393. [[CrossRef](#)] [[PubMed](#)]
- Ahmad, T.; Danish, M.; Rafatullah, M.; Ghazali, A.; Sulaiman, O.; Hashim, R.; Ibrahim, M.N.M. The use of date palm as a potential adsorbent for wastewater treatment: A review. *Environ. Sci. Pollut. Res.* **2012**, *19*, 1464–1468. [[CrossRef](#)]
- Lee, C.G.; Lee, S.; Park, J.A.; Park, C.; Lee, S.J.; Kim, S.B.; An, B.; Yun, S.T.; Lee, S.H.; Choi, J.W. Removal of copper, nickel and chromium mixtures from metal plating wastewater by adsorption with modified carbon foam. *Chemosphere* **2017**, *166*, 203–211. [[CrossRef](#)]
- Prithviraj, D.; Deboleena, K.; Neelu, N.; Noor, N.; Aminur, R.; Balasaheb, K.; Abul, M. Biosorption of nickel by *Lysinibacillus* sp. BA2 native to bauxite mine. *Ecotoxicol. Environ. Saf.* **2014**, *107*, 260–268. [[CrossRef](#)]
- Salem, N.M.; Awwad, A.M. Biosorption of Ni(II) from electroplating wastewater by modified (*Eriobotrya japonica*) loquat bark. *J. Saudi Chem. Soc.* **2014**, *18*, 379–386. [[CrossRef](#)]
- Onundi, Y.B.; Mamun, A.A.; Al Khatib, M.F.; Ahmed, M. Adsorption of copper, nickel and lead ions from synthetic semiconductor industrial wastewater by palm shell activated carbon. *Int. J. Environ. Sci. Technol.* **2010**, *7*, 751–758. [[CrossRef](#)]
- Alomá, I.; Martín-Lara, M.A.; Rodríguez, I.L.; Blázquez, G.; Calero, M. Removal of nickel (II) ions from aqueous solutions by biosorption on sugarcane bagasse. *J. Taiwan Inst. Chem. Eng.* **2012**, *43*, 275–281. [[CrossRef](#)]
- El Marouani, M.; Azoulay, K.; Bencheikh, I.; Elfakir, L.; Rghioui, L.; El Hajji, A.; Sebbahi, S.; El Hajjaji, S.; Kifani-Sahban, F. Application of raw and roasted date seeds for dyes removal from aqueous solution. *J. Mater. Environ. Sci.* **2018**, *9*, 2387–2396.
- Chang, Y.S.; Au, P.I.; Mubarak, N.M.; Khalid, M.; Jagadish, P.; Walvekar, R.; Abdullah, E.C. Adsorption of Cu(II) and Ni(II) ions from wastewater onto bentonite and bentonite/GO composite. *Environ. Sci. Pollut. Res.* **2020**, *27*, 33270–33296. [[CrossRef](#)] [[PubMed](#)]
- Mehrmad, N.; Moravegi, M.; Parvareh, A. Adsorption of Pb(II), Cu(II) and Ni(II) ions from aqueous solutions by functionalised henna powder (*Lawsonia Inermis*); isotherm, kinetic and thermodynamic studies. *Int. J. Environ. Anal. Chem.* **2020**. [[CrossRef](#)]
- Khan, M.I.; Almesfer, M.K.; Danish, M.; Ali, I.H.; Shoukry, H.; Patel, R.; Gardy, J.; Nizami, A.S.; Rehan, M. Potential of Saudi natural clay as an effective adsorbent in heavy metals removal from wastewater. *Desalin. Water Treat.* **2019**, *158*, 140–151. [[CrossRef](#)]

14. Bartczak, P.; Norman, M.; Klapiszewski, L.; Karwan'ska, N.; Kawalec, M.; Baczyn'ska, M.; Wysokowski, M.; Zdarta, J.; Ciesielczyk, F.; Jesionowski, T. Removal of nickel(II) and lead(II) ions from aqueous solution using peat as a low-cost adsorbent: A kinetic and equilibrium study. *Arab. J. Chem.* **2018**, *11*, 1209–1222. [[CrossRef](#)]
15. Ali, I.H.; Al Mesfer, M.K.; Khan, M.I.; Danish, M.; Alghamdi, M.M. Exploring Adsorption Process of Lead (II) and Chromium (VI) Ions from Aqueous Solutions on Acid Activated Carbon Prepared from *Juniperus procera* Leaves. *Processes* **2019**, *7*, 217. [[CrossRef](#)]
16. Chang, C.F.; Chang, C.Y.; Chen, K.H.; Tsai, W.T.; Shie, J.L.; Chen, Y.H. Adsorption of naphthalene on zeolite from aqueous solution. *J. Colloid. Interface Sci.* **2004**, *277*, 29–34. [[CrossRef](#)]
17. Ali, I.H.; Sulfab, Y. Kinetics and mechanism of oxidation of cisdiaquabis(glycinato)chromium(III) by periodate ion in aqueous solutions. *Transit. Met. Chem.* **2013**, *38*, 79–84. [[CrossRef](#)]
18. Tempkin, M.I.; Pyzhev, V. Kinetic of Ammonia Synthesis on Promoted Iron Catalyst. *Acta Phys. Chim. USSR* **1940**, *12*, 327–356.
19. Günay, A.; Arslankaya, E.; Tosun, I. Lead removal from aqueous solution by natural and pretreated clinoptilolite: Adsorption equilibrium and kinetics. *J. Hazard. Mater.* **2007**, *146*, 362–371. [[CrossRef](#)]
20. Gupta, S.; Kumar, A. Removal of nickel (II) from aqueous solution by biosorption on *A. barbadensis* Miller waste leaves powder. *Appl. Water Sci.* **2019**, *9*, 96–107. [[CrossRef](#)]
21. Priyantha, N.; Kotabewatta, P.A. Biosorption of heavy metal ions on peel of *Artocarpus nobilis* fruit: 1—Ni(II) sorption under static and dynamic conditions. *Appl. Water Sci.* **2019**, *9*, 37–47. [[CrossRef](#)]
22. Gupta, S.; Sharma, S.K.; Kumar, A. Biosorption of Ni(II) ions from aqueous solution using modified *Aloe barbadensis* Miller leaf powder. *Water Sci. Eng.* **2019**, *12*, 27–36. [[CrossRef](#)]
23. Barquilha, C.E.R.; Cossich, E.S.; Tavares, C.R.; Silva, E.A. Biosorption of nickel(II) and copper(II) ions by *Sargassum* sp. in nature and alginate extraction products. *Bioresour. Technol. Rep.* **2019**, *5*, 43–50. [[CrossRef](#)]
24. Pandey, P.K.; Choubey, S.; Verma, Y.; Pandey, M.; Kamal, S.S.; Chandrashekhar, K. Biosorptive removal of Ni(II) from wastewater and industrial effluent. *Int. J. Environ. Res. Public Health* **2007**, *4*, 332–339. [[CrossRef](#)] [[PubMed](#)]
25. Thevannan, A.; Mungroo, R.; Niu, C. Biosorption of nickel with barley straw. *Bioresour. Technol.* **2010**, *101*, 1776–1780. [[CrossRef](#)]
26. Feng, N.; Guo, X.; Liang, S.; Zhu, Y.; Liu, J. Biosorption of heavy metals from aqueous solutions by chemically modified orange peel. *J. Hazard. Mater* **2011**, *185*, 49–54. [[CrossRef](#)]
27. Malkoc, E.; Nuhoglu, Y. Investigations of nickel(II) removal from aqueous solutions using tea factory waste. *J. Hazard. Mater* **2005**, *127*, 120–128. [[CrossRef](#)]



© 2020 by the authors. Licensee MDPI, Basel, Switzerland. This article is an open access article distributed under the terms and conditions of the Creative Commons Attribution (CC BY) license (<http://creativecommons.org/licenses/by/4.0/>).